

A power law solution for Bianchi-I Universe with observational constraints

Lokesh Kumar Sharma,^{1,*} Suresh Parekh,^{2,†} Kalyani C.K. Mehta,^{3,‡} Saibal Ray,^{4,§} and Anil Kumar Yadav^{5,¶}

¹*Department of Physics, GLA University, Mathura 281406, Uttar Pradesh, India*

²*Department of Physics, SP Pune University, Pune 411007, Maharashtra, India*

³*Department of Physics, Eberhard Karls University of Tübingen, Germany*

⁴*Center for Cosmology, Astrophysics and Space Science (CCASS),
GLA University, Mathura 281406, Uttar Pradesh, India*

⁵*Department of Physics, United College of Engineering and Research, Greater Noida 201 306, India*

(Dated: November 29, 2023)

We have studied a dark energy dominating bulk viscous universe in Bianchi type I space-time and limited its parameter using observational $H(z)$ data (OHD), combined OHD and BAO, and Pantheon's collection of SN Ia data in this study. We have used the 57-point $H(z)$ data, 8-point BAO data, 1048-point Pantheon data, joint data of $H(z)$ + Pantheon, and joint data of $H(z)$ + BAO + Pantheon and obtained the model parameters α , β , H_0 by using the Markov Chain Monte Carlo (MCMC) method. The constrained values of the model parameter are as follows: $H_0 = 69.860^{+2.431}_{-2.111}$ km s⁻¹ Mpc⁻¹, $H_0 = 70.921^{+2.069}_{-2.385}$ km s⁻¹ Mpc⁻¹, $H_0 = 69.320^{+2.261}_{-2.112}$ km s⁻¹ Mpc⁻¹, $H_0 = 68.912^{+2.097}_{-1.921}$ km s⁻¹ Mpc⁻¹, $H_0 = 69.460^{+2.064}_{-2.284}$ km s⁻¹ Mpc⁻¹ respectively. These computed H_0 observational values agree well with the outcomes from the Planck collaboration group. Through an analysis of the energy conditions' behavior on our obtained solution, the model has been examined and analysed. Using the Om diagnostic as the state finder diagnostic tool and the jerk parameter, we have also investigated the model's validity. Our results show that, within a certain range of restrictions, the proposed model agrees with the observed signatures.

I. INTRODUCTION

The concept of late time cosmic acceleration has been validated by SN Ia observations in the final decade of the twentieth century [1]. We can improve the cosmic model by using these observations. An estimated 95% of the universe's energy, sometimes referred to as dark energy or dark matter, remains a mystery according to modern cosmological models [2]. Planck team constraints reveal a distribution of dark matter and dark energy in the ratio of 1 : 2.8 [3]. One of the biggest problems in modern physics is that particle physics experiments have not yet produced a good physical candidate for the universe's dark matter and dark energy components. Two significant theoretical issues plague the cosmological constant (Λ), the dark energy candidate most often cited, namely cosmic coincidence and fine tuning. Consequently, teleparallel gravity is one of several modifications to general theory of relativity that have been put up in the literature, $f(R)$ and $f(R, T)$ gravity [19]. A Ricci scalar and a trace of energy momentum tensor are related to the matter Lagrangian in $f(R, T)$ gravity [6–11, 16]. Given the T -dependence of $f(R, T)$ gravity, it is possible to think about quantum effects, which in turn give the chances of particle generation [12]. By taking into account a relationship between matter and geometry, these possibilities may provide a hint that

the extended theory of gravity and quantum theory of gravity are related. More and more people are looking at the $f(R, T)$ theory of gravity recently since it unifies the available data, passes the local tests, and describes the phase shift from a matter-dominated to a dark energy/dark matter dominated world [13, 14]. Kiani and Nozari looked at the $f(R, T)$ model that characterised the space-time scalar perturbation [15]. A non-minimal matter-geometry coupling for the FRW model of the universe, controlled by a hybrid expansion law, has been recently established by Sahoo and Moraes [16].

According to the authors, the simplest explanation for the coupling of matter with higher-order derivative curvature is the transfer of momentum and energy. As a result, the second law of thermodynamics is satisfied, and the geometric curvature transforms into matter, and an irreversible flow from the gravitational field of the newly formed matter constituent occurs [17]. $f(R, T)$ theories seem to be a viable alternative to dark matter, and they pass the solar system test [18].

II. THE METRIC AND $f(R, T) = f_1(R) + f_2(R)f_3(T)$ GRAVITY

Bianchi type -I space-time is read as

$$ds^2 = -c^2 dt^2 + X^2 dx^2 + Y^2 dy^2 + Z^2 dz^2 \quad (1)$$

Here, $X(t)$, $Y(t)$, $Z(t)$ are scale factor along x, y and z -direction.

The action in $f(R, T)$ gravity is given by

$$S = \frac{1}{16\pi} \int d^4x \sqrt{-g} f(R, T) + \int d^4x \sqrt{-g} L_m \quad (2)$$

*Email: lokesh.sharma@gla.ac.in

†Email: thesureshparekh@gmail.com

‡Email: kalyani.c.k.mehta@gmail.com

§Email: saibal.ray@gla.ac.in

¶Email: abanilyadav@yahoo.co.in

where g and L_m are the metric determinant and matter Lagrangian density respectively.

The gravitational field of $f(R, T)$ gravity is given by

$$\begin{aligned} & [f'_1(R) + f'_2(R)f'_3(T)] R_{ij} \\ & - \frac{1}{2}f'_1(R)g_{ij} \\ & + (g_{ij}\nabla^i\nabla_j - \nabla_i\nabla_j)[f'_1(R) + f'_2(R)f'_3(T)] \\ & = [8\pi + f'_2(R)f'_3(T)]T_{ij} \\ & = +f_2(R)\left[f'_3(T)p + \frac{1}{2}f_3(T)\right]g_{ij} \end{aligned} \quad (3)$$

Here, $f(R, T) = f_1(R) + f_2(R)f_3(T)$ and primes denote derivatives with respect to the arrangement.

We assume $f_1(R) = f_2(R) = R$ and $f_3(T) = \alpha T$, with α as a constant. Thus the equation (3) yields

$$G_{ij} = 8\pi T_{ij}^{(eff)} = 8\pi(T_{ij} + T_{ij}^{DE}) \quad (4)$$

where, $T_{ij}^{(eff)}$, T_{ij} and T_{ij}^{DE} represent the effective energy momentum tensor, matter energy momentum tensor and dark energy term respectively. The dark energy term is read as

$$T_{ij}^{DE} = \frac{\alpha R}{8\pi} \left(T_{ij} + \frac{3\rho - 7p}{2} g_{ij} \right) \quad (5)$$

By applying the Bianchi identities in equation (II) yields

$$\nabla^i T_{ij} = -\frac{\alpha R}{8\pi} \left[\nabla^i(T_{ij} + pg_{ij}) + \frac{1}{2}g_{ij}\nabla^i(\rho - 3p) \right] \quad (6)$$

III. THE $f(R, T) = R + \alpha RT$ COSMOLOGY

For the line element (1), the field equation (4) can be written as

$$\frac{\ddot{Y}}{Y} + \frac{\ddot{Z}}{Z} + \frac{\dot{Y}\dot{Z}}{YZ} = -8\pi p^{(eff)} \quad (7)$$

$$\frac{\ddot{Z}}{Z} + \frac{\ddot{X}}{X} + \frac{\dot{X}\dot{Z}}{XZ} = -8\pi p^{(eff)} \quad (8)$$

$$\frac{\ddot{X}}{X} + \frac{\ddot{Y}}{Y} + \frac{\dot{X}\dot{Y}}{XY} = -8\pi p^{(eff)} \quad (9)$$

$$\frac{\dot{X}\dot{Y}}{XY} + \frac{\dot{Y}\dot{Z}}{YZ} + \frac{\dot{Z}\dot{X}}{ZX} = 8\pi\rho^{(eff)} \quad (10)$$

Here, $\rho^{(eff)} = \rho + \rho^{(de)} = \rho - \frac{3\alpha}{8\pi} \left(\frac{\ddot{a}}{a} + \frac{\dot{a}^2}{a^2} \right) (3\rho - 7p)$, $p^{(eff)} = p + p^{(de)} = p + \frac{9\alpha}{8\pi} \left(\frac{\ddot{a}}{a} + \frac{\dot{a}^2}{a^2} \right) (\rho - 3p)$ and $a = (XYZ)^{\frac{1}{3}}$ is average scale factor.

The above equations (7)-(10) can also be written as

$$\frac{(XYZ)^\cdot}{XYZ} = 12\pi(\rho^{(eff)} - p^{(eff)}) \quad (11)$$

We define Hubble's parameter (H) in connection with average scale factor as follow:

$$H = \frac{\dot{a}}{a} \quad (12)$$

Applying a special law of variation of Hubble's parameter that yield the power law expansion of scale factor i.e.

$$a = (nDt)^{\frac{1}{n}} \quad (13)$$

where n & D are non zero positive constants and the integrating constant has been omitted by assuming that $a = 0$ at $t = 0$.

IV. OBSERVATIONAL ANALYSIS: CONSTRAINTS ON MODEL PARAMETERS

In this Section, we try to limit the model parameters H_0 , α and β with reference to the observationally obtained $H(z)$ dataset under the redshift range $0 \leq z \leq 1.965$. The $H(z)$ observational dataset is provided in the references. Moreover, the scaling factor with respect to redshift is given by

$$a = \frac{a_0}{z+1} = \alpha t^\beta, \quad (14)$$

where a_0 denotes the present value of the scale factor.

The age of the Universe is computed with the following equation

$$H(z) = -\frac{1}{z+1} \frac{dz}{dt}. \quad (15)$$

Putting together Eqs. (14 - 15) and there after a bit manipulation, we can easily get the following Hubble parameter in its functional form as

$$H(z) = \beta \left(\frac{a_0}{\alpha} \right)^{-\frac{1}{\beta}} (z+1)^{\frac{1}{\beta}} \quad (16)$$

From Eq. (16), the present value of the Hubble constant is determined as $H_0 = \beta \left(\frac{a_0}{\alpha} \right)^{-\frac{1}{\beta}}$.

Let us now confine the model parameters, viz. H_0 , α and β to the redshift range $0 \leq z \leq 1.965$ by using the observable $H(z)$, BAO and Pantheon datasets. The distribution of the datasets for the observational aspect of $H(z)$ is shown in 1 and the data points are listed in ???. The details for BAO and Pantheon are taken from ref. [20].

TABLE I: Parameter values obtained from different datasets after running MCMC and Bayesian analysis where t_C is the age of the Universe (Gyr) with the notations as $H(z)_1 = H(z) + \text{Pantheon}$ and $H(z)_2 = H(z) + \text{Pantheon} + \text{BAO}$

Parameter	$H(z)$	BAO	Pantheon	$H(z)_1$	$H(z)_2$
H_0	$69.860^{+2.431}_{-2.111}$	$70.921^{+2.069}_{-2.385}$	$69.320^{+2.261}_{-2.112}$	$68.912^{+2.097}_{-1.921}$	$69.460^{+2.064}_{-2.284}$
α	$69.992^{+0.089}_{-0.089}$	$70.034^{+0.087}_{-0.121}$	$69.993^{+0.096}_{-0.092}$	$70.023^{+0.095}_{-0.099}$	$69.997^{+0.119}_{-0.087}$
β	$1.001^{+0.010}_{-0.010}$	$0.996^{+0.010}_{-0.008}$	$1.003^{+0.009}_{-0.010}$	$1.005^{+0.009}_{-0.009}$	$1.002^{+0.011}_{-0.009}$
t_C	14.328657	14.043795	14.469128	14.583817	14.425568

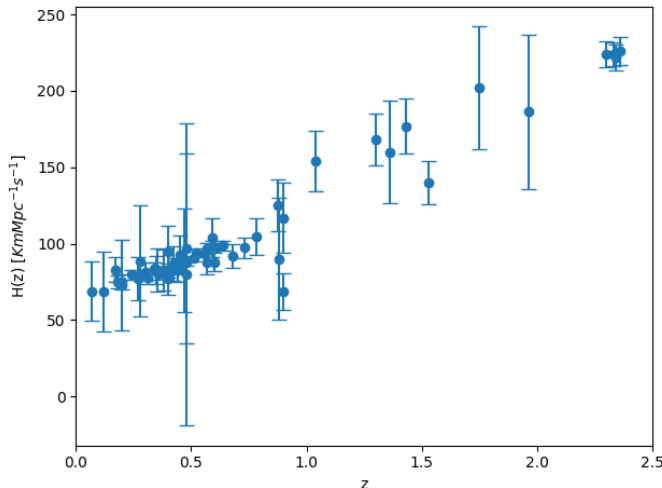


FIG. 1: Error bar plot of the 57 point $H(z)$ data used in analysis of our model

V. PHYSICAL PARAMETERS AND DIAGNOSTIC ANALYSIS

A. Energy Conditions

Energy conditions (ECs) are like the cosmic rules that help us to understand that the universe (energy as well as matter) distributes throughout the universe. They are based on the Einstein equations of gravity and serve as the laws of the cosmos. These conditions reveal the distribution of the energy and matter in space.

1. Weak Energy Condition (WEC): The WEC says that the energy cannot be negative or zero anywhere in the universe. This condition helps us keep the universe's rules fair and consistent. Figure 16 shows the nature of WEC for our model using the parameters obtained in the Bayesian Analysis.
2. Null Energy Condition (NEC): The NEC is about light, which states that when light travels through the universe, it always encounters some energy. This condition keeps the universe's physics sensible and prevents strange things from happening. Figure 13 shows the nature of NEC for our model using the parameters obtained in the Bayesian Analysis.

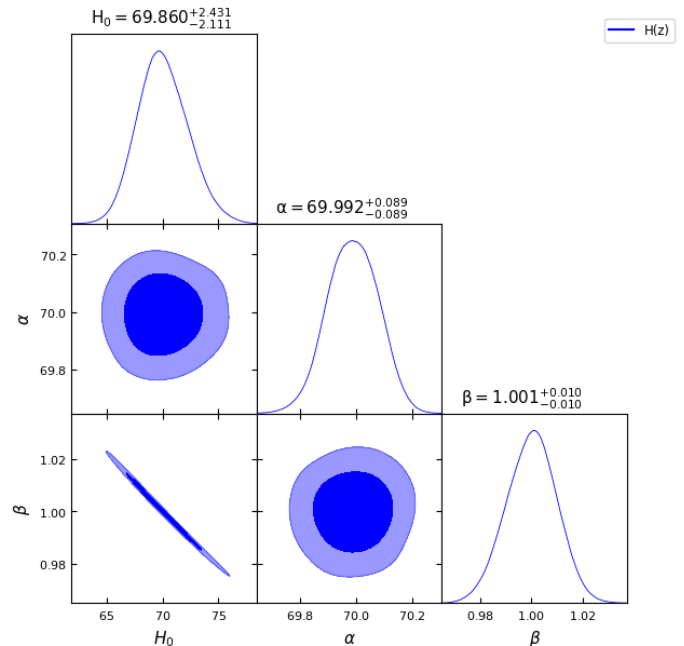


FIG. 2: One-dimensional marginalized distribution and two-dimensional contours for our $f(R, T)$ model parameters H_0 , α , β using the $H(z)$ dataset presented in Table ??

3. Strong Energy Condition (SEC): The SEC is like a stricter version of the NEC. It ensures that energy cannot be negative and limits how things behave under gravity. It is like saying gravity always pulls things together; it cannot push them apart. This rule helps maintain order in the universe. Figure 15 shows the nature of SEC for our model using the parameters obtained in the Bayesian Analysis.
4. Dominant Energy Condition (DEC): The DEC builds on the NEC and ensures that energy is not only non-negative but that how energy flows around cannot be too wild. It is like saying that energy cannot move faster than light or get too crazy. This condition ensures that the universe does not have any weird surprises. Figure 14 shows the nature of DEC for our model using the parameters obtained in the Bayesian Analysis.

All the above-mentioned energy conditions are com-

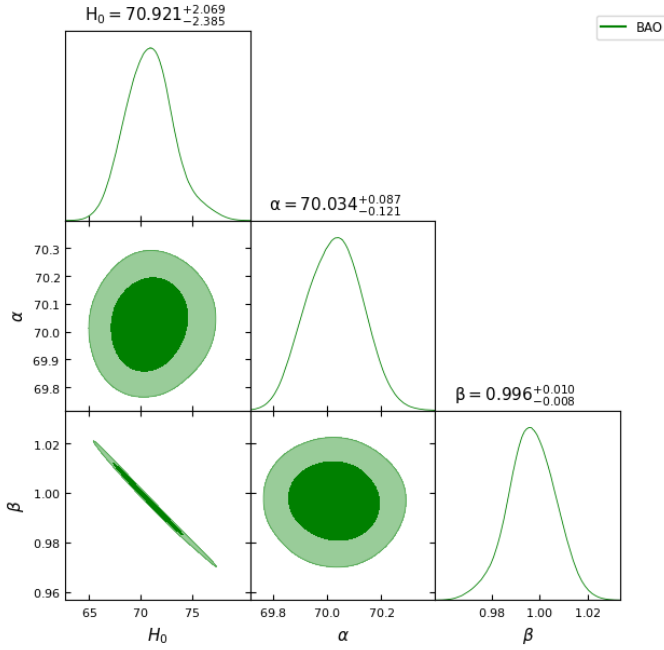


FIG. 3: One-dimensional marginalized distribution and two-dimensional contours for our $f(R, T)$ model parameters H_0 , α and β using the BAO dataset ref. [20]

bin in Fig. 9 whereas the energy condition relations are as shown mathematically below [21, 22]:

$$\text{NEC} : \rho + p \geq 0, \quad (17)$$

$$\text{WEC} : \rho + p \geq 0 \ \& \ \rho \geq 0, \quad (18)$$

$$\text{SEC} : \rho + p \geq 0 \ \& \ \rho + 3p \geq 0, \quad (19)$$

$$\text{DEC} : \rho - p \geq 0 \ \& \ \rho \geq 0. \quad (20)$$

Fig. 10 displays the energy density distribution ρ with respect to time t , whereas Fig. 11 illustrates the pressure p . Our results demonstrate that all other energy conditions i.e., NEC, WEC, and DEC, are met, except the SEC. The universe's growing rate supports the SEC violation. Consequently, the late-time acceleration of the present universe may be satisfactorily explained by the $f(R, T)$ theory of gravity, which benefits from the trace energy T contribution without requiring the presence of dark energy or the cosmological constant in the universe's energy content.

B. State finder diagnostic

State Finder Diagnostics are like cosmic detectives helping us unravel the mysteries of dark energy and the universe's evolution. These diagnostics are like a cosmic compass, guiding us through the complexities of cosmic evolution. State Finder Diagnostics build upon the two key parameters r and s . These parameters help us understand how the universe is changing over time. One can think of them as the cosmic meters that tell us

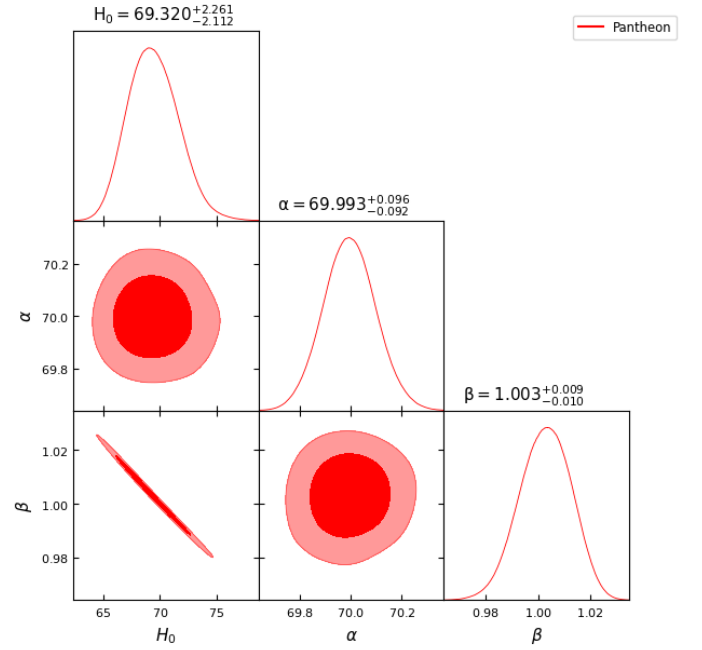


FIG. 4: One-dimensional marginalized distribution and two-dimensional contours for our $f(R, T)$ model parameters H_0 , α and β using the Pantheon dataset ref. [20]

about the universe's expansion and the stuff that makes it up. They are dimensionless parameters that encapsulate the essence of the universe's solution, providing a lens through which we discern the universe's underlying dynamics. The general mathematical parametric definitions of these factors are as follows:

$$r = \frac{\ddot{a}}{aH^3}, r = \frac{(-1 + r)}{3(-\frac{1}{2} + q)}. \quad (21)$$

However, the equations for r and s in our model which are expressed in terms of q , can be obtained as follows:

$$r = q(1 + 2q),$$

$$s = \frac{2}{3}(q + 1).$$

Figure 17 has demonstrated that the scale factor trajectories in the derived model follow a particular set of routes. Our approach corresponds to the outcomes obtained from the power law cosmology for the cosmic diagnostic pair.

C. Om(z) parameter

Researchers typically use the state finder parameters $r - s$ and do analysis using the Om diagnostic to look at different dark energy theories in their academic works. The Hubble parameter H and the cosmic redshift z combine to generate the $Om(z)$ parameter, which is essential.

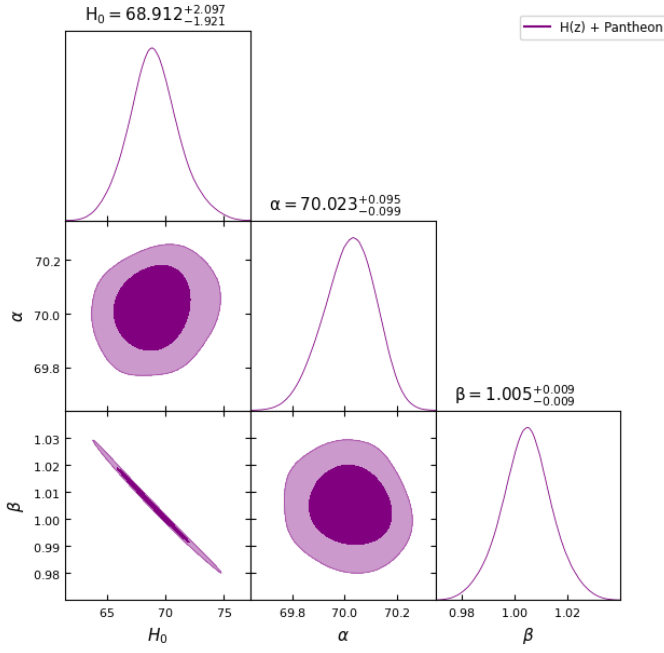


FIG. 5: One-dimensional marginalized distribution and two-dimensional contours for our $f(R, T)$ model parameters H_0 , α and β using the combination of $H(z)$ and Pantheon dataset

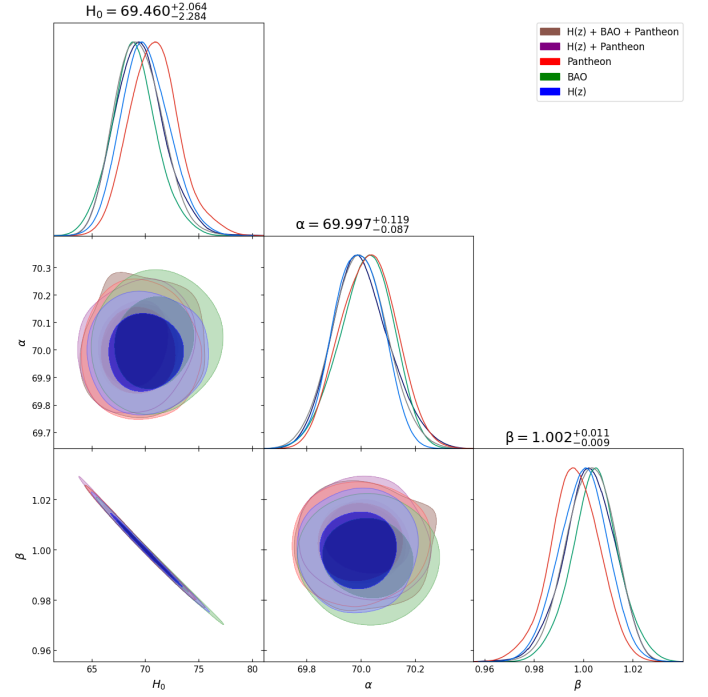


FIG. 7: One-dimensional marginalized distributions and two-dimensional contours representing our $f(R, T)$ model parameters H_0 , α and β , depicting the combined variability across all dataset combinations

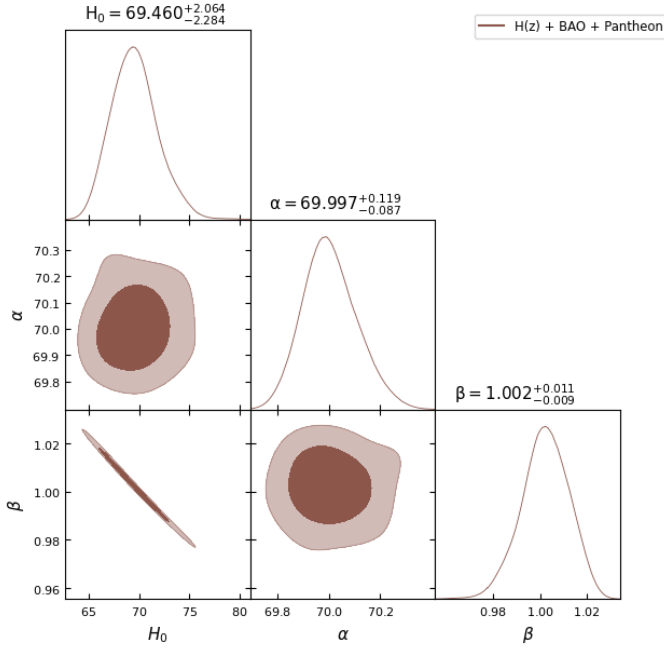


FIG. 6: One-dimensional marginalized distribution and two-dimensional contours for our $f(R, T)$ model parameters H_0 , α and β using the combination of $H(z)$, BAO and Pantheon dataset

Initially, Sahni et al. [23] and later on others [24–26] offer the $Om(z)$ parameter formula in the context of changed gravity as follows:

$$Om(z) = \frac{\left[\frac{H(z)}{H_0}\right]^2 - 1}{(1+z)^3 - 1}. \quad (22)$$

Here, the Hubble parameter is denoted by H_0 . According to Shahalam et al. [27], the quintessence ($\omega \geq -1$), Λ CDM and phantom ($\omega \leq -1$) dark energy (DE) models are represented by the negative, zero and positive values of $Om(z)$, respectively. We obtain the $Om(z)$ parameter for the present model as follows:

$$Om(z) = \frac{(1+z)^{2/b} - 1}{(1+z)^3 - 1}. \quad (23)$$

D. Jerk Parameter

The Hubble parameter, the deceleration parameter, and the jerk parameter - all offer profound insights into cosmic evolution. The jerk parameter, denoted as j , measures how the universe's acceleration changes over time. [24]. A positive j ($j \geq 0$) means that the universe's acceleration is speeding up, which means it is getting faster. On the other hand, a negative j ($j \leq 0$) implies the acceleration is slowing down. Various dark energy theories

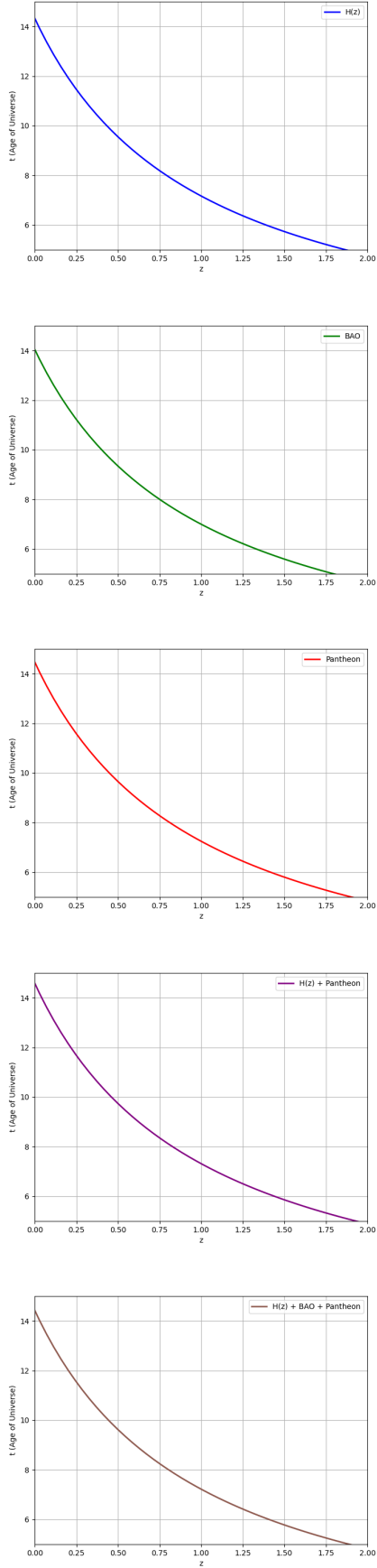


FIG. 8: Graphical representation of cosmic time over redshift. It is crucial for understanding cosmic evolution and validating cosmological models. Five plots are for different combinations of $H(z)$, BAO and Pantheon datasets. The age of the Universe (t_C) at $z = 0$ are mentioned in the Table I

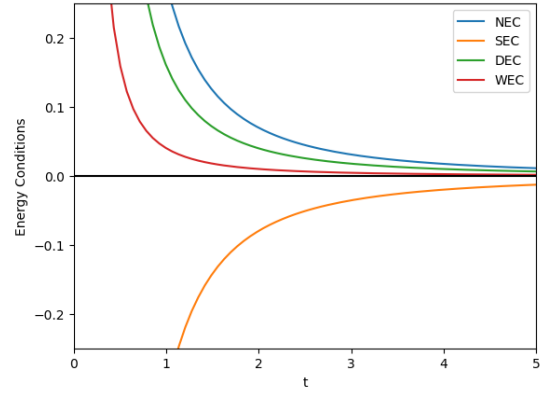


FIG. 9: Visualisation of all Energy Conditions vs time

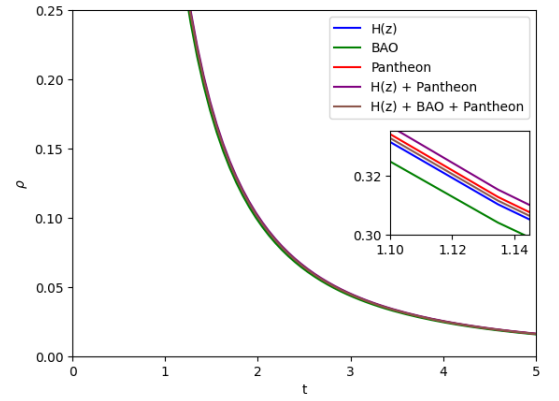


FIG. 10: Graphical representation illustrates the dynamic variation of the energy density (ρ) over the time (t) under various parameter conditions derived from distinct combinations of the $H(z)$, BAO and Pantheon datasets

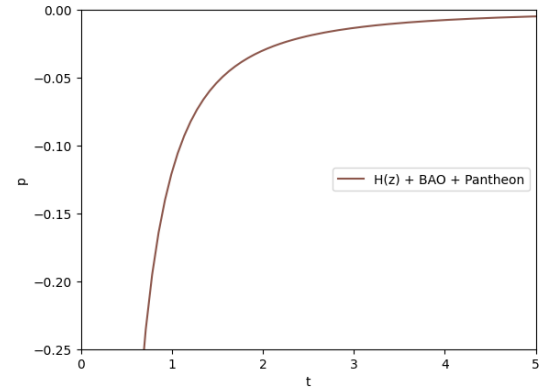


FIG. 11: Graphical representation illustrates the dynamic variation of the pressure p over time (t) under various parameter conditions derived from distinct combinations of the $H(z)$, BAO and Pantheon datasets

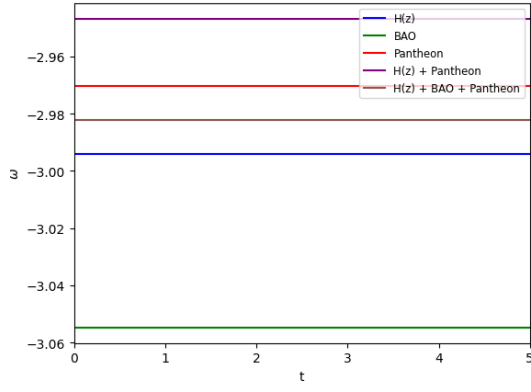


FIG. 12: Plot of variation of Equation of State parameter ω vs time t . The plot suggests that dark energy contributes to the universe's accelerated expansion but with some variations over time, potentially leading to interesting cosmological consequences.

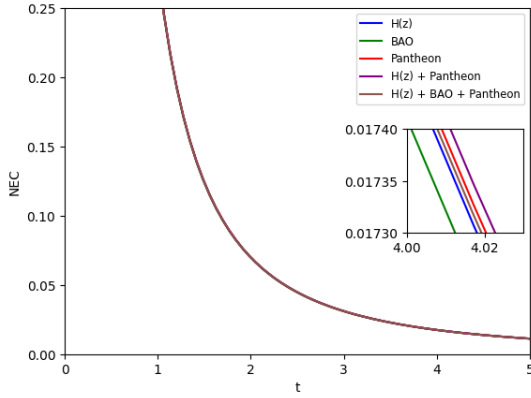


FIG. 13: Visualisation of null energy condition (NEC) vs time for all dataset combinations.

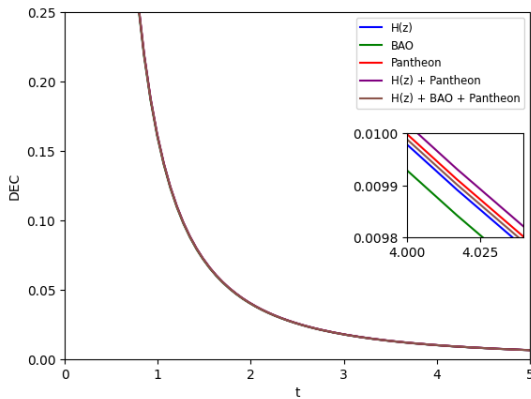


FIG. 14: Visualisation of the dominant energy condition (DEC) vs time for all dataset combinations.

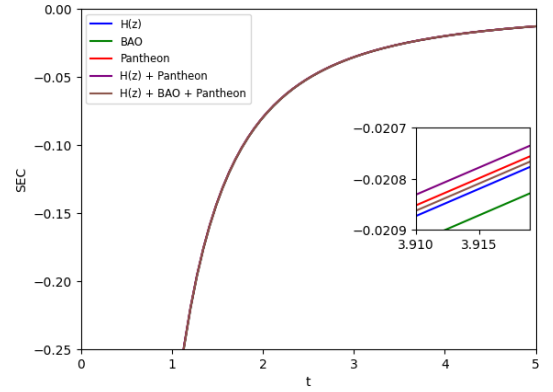


FIG. 15: Visualisation of the strong energy conditions (SEC) vs time for all dataset combinations.

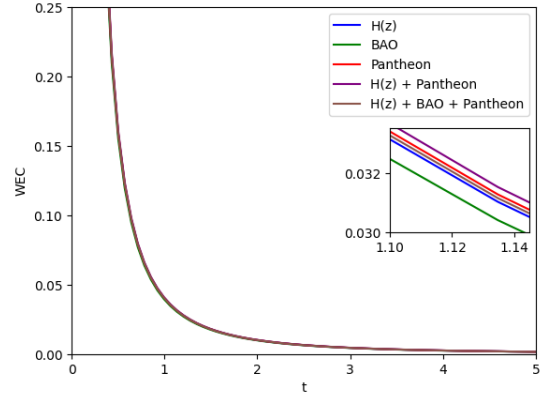


FIG. 16: Visualisation of the weak energy conditions (WEC) vs time for all dataset combinations.

predict different values for the jerk parameter. By measuring j and comparing it to these predictions, scientists can get clues about the nature of the dark energy, which is supposed to be the mysterious force driving the universe's acceleration. When combined with other cosmic parameters, the jerk parameter helps improve our models of the universe. It rigorously tests these models, ensuring they accurately match what we observe in the real universe. For our model, we have obtained parameters, especially the variation of j w.r.t the redshift z , which is shown in Fig. 19.

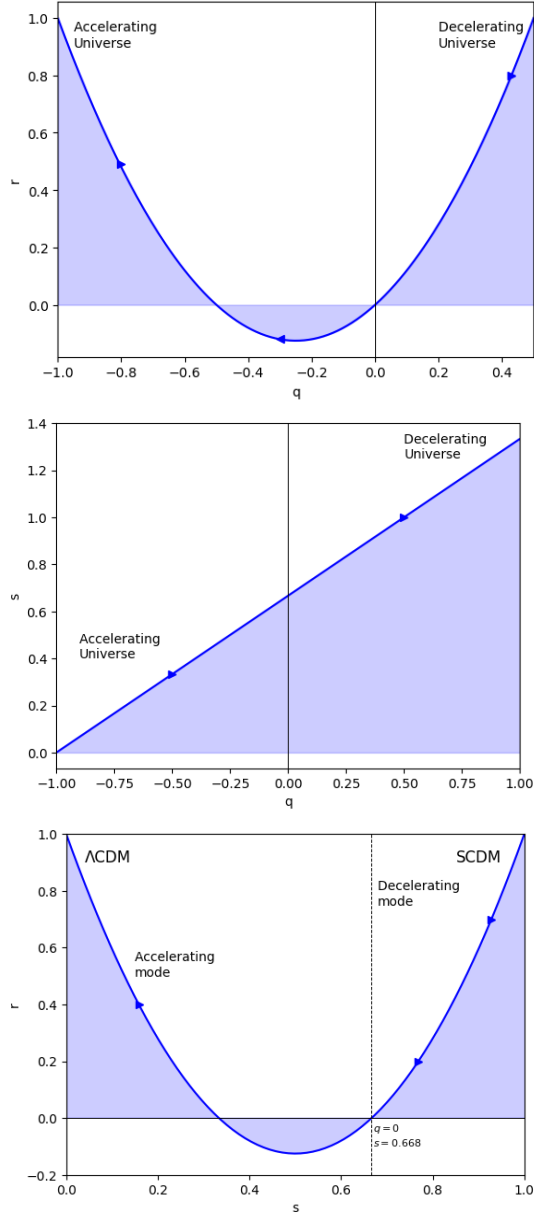


FIG. 17: State finder plots of $r - q$, $s - q$ and $r - s$.

VI. CONCLUSION

Acknowledgements

S. Ray acknowledges support from the Inter-University Centre for Astronomy and Astrophysics (IUCAA), Pune, India, under the Visiting Research Associateship Programme and facilities under ICARD, Pune at CCASS, GLA University, Mathura, India. L.K. Sharma is thankful to IUCAA for approving a short visit when the idea of the present work has been conceived.

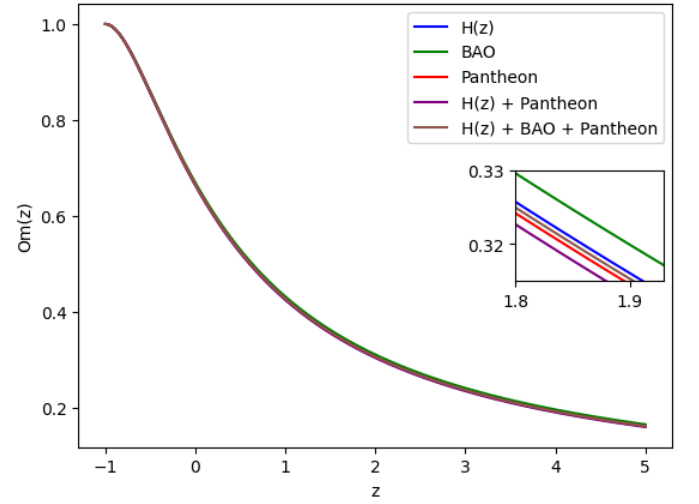


FIG. 18: Examining the variations of $Om(z)$ with z across different dataset combinations, considering the β values obtained from each dataset.

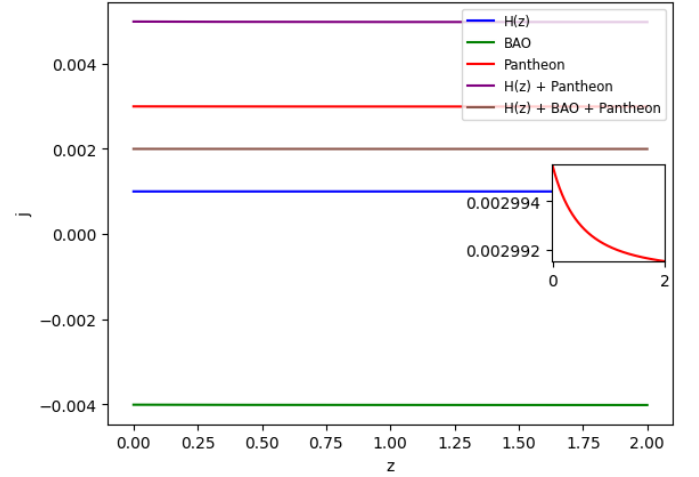


FIG. 19: Visualisation of Jerk parameter j vs z . Values of Jerk parameter at $z = 0$ are, for $H(z) = 0.0009 \text{ s}^{-3}$, for $BAO = -0.004 \text{ s}^{-3}$, for $Pantheon = 0.0029 \text{ s}^{-3}$, for $H(z)_1 = H(z) + Pantheon = 0.0049 \text{ s}^{-3}$ and for $H(z)_2 = H(z) + BAO + Pantheon = 0.0019 \text{ s}^{-3}$.

Data Availability Statement

In this manuscript, we have used observational data as available in the literature. [Authors' comment: Our work does not produce any form of new data.]

Conflicts of Interest

The authors assert that there are no conflicts of interest pertaining to the publication of this work.

-
- [1] S. Perlmutter *et al.* [Supernova Cosmology Project], “Measurements of Ω and Λ from 42 high redshift supernovae,” *Astrophys. J.* **517**, 565-586 (1999)
- [2] S. Kumar and R. C. Nunes, “Observational constraints on dark matter–dark energy scattering cross section,” *Eur. Phys. J. C* **77**, no.11, 734 (2017)
- [3] P. A. R. Ade *et al.* [Planck], “Planck 2015 results. XV. Gravitational lensing,” *Astron. Astrophys.* **594**, A15 (2016)
- [4] Harko, Tiberiu, Francisco SN Lobo, Shinâichi Nojiri, and Sergei D. Odintsov. “ $f(R, T)$ gravity.” *Physical Review D* **84**, no. 2 (2011): 024020.
- [5] P. H. R. S. Moraes and P. K. Sahoo, “The simplest non-minimal matter-geometry coupling in the $f(R, T)$ cosmology,” *Eur. Phys. J. C* **77**, no.7, 480 (2017)
- [6] A. Kumar Yadav, “Bianchi-V string cosmology with power law expansion in $f(R, T)$ Gravity,” *Eur. Phys. J. Plus* **129**, 194 (2014)
- [7] Yadav, Anil Kumar, and Ahmad T. Ali. “Invariant Bianchi type I models in $f(R, T)$ gravity.” *International Journal of Geometric Methods in Modern Physics* **15**, no. 02 (2018): 1850026.
- [8] A. K. Yadav, L. K. Sharma, B. K. Singh and P. K. Sahoo, “Existence of bulk viscous universe in $f(R, T)$ gravity and confrontation with observational data,” *New Astron.* **78**, 101382 (2020)
- [9] L. K. Sharma, A. K. Yadav and B. K. Singh, “Power-law solution for homogeneous and isotropic universe in $f(R, T)$ gravity,” *New Astron.* **79**, 101396 (2020)
- [10] L. K. Sharma, B. K. Singh and A. K. Yadav, “Viability of Bianchi type V universe in $f(R, T) = f_1(R) + f_2(R)f_3(T)$ gravity,” *Int. J. Geom. Meth. Mod. Phys.* **17**, no.07, 2050111 (2020)
- [11] L. K. Sharma, A. K. Yadav, P. K. Sahoo and B. K. Singh, “Non-minimal matter-geometry coupling in Bianchi I space-time,” *Results Phys.* **10**, 738-742 (2018)
- [12] L. Parker, “Quantized fields and particle creation in expanding universes. 2,” *Phys. Rev. D* **3**, 346-356 (1971)
- [13] R. Myrzakulov, “FRW Cosmology in $F(R, T)$ gravity,” *Eur. Phys. J. C* **72**, 2203 (2012)
- [14] S. K. Sahu, S. K. Tripathy, P. K. Sahoo and A. Nath, “Cosmic Transit and Anisotropic Models in $f(R, T)$ Gravity,” *Chin. J. Phys.* **55**, 862-869 (2017)
- [15] F. Kiani and K. Nozari, “Energy conditions in $F(T, \Theta)$ gravity and compatibility with a stable de Sitter solution,” *Phys. Lett. B* **728**, 554-561 (2014)
- [16] P. H. R. S. Moraes and P. K. Sahoo, “The simplest non-minimal matter-geometry coupling in the $f(R, T)$ cosmology,” *Eur. Phys. J. C* **77**, no.7, 480 (2017)
- [17] T. Harko, F. S. N. Lobo, J. P. Mimoso and D. Pavón, “Gravitational induced particle production through a nonminimal curvature–matter coupling,” *Eur. Phys. J. C* **75**, 386 (2015)
- [18] R. Zaregonbadi, M. Farhoudi and N. Riazi, “Dark Matter From $f(R, T)$ Gravity,” *Phys. Rev. D* **94**, 084052 (2016)
- [19] Harko, Tiberiu, Francisco SN Lobo, Shinâichi Nojiri, and Sergei D. Odintsov. “ $f(R, T)$ gravity.” *Physical Review D* **84**, no. 2 (2011): 024020.
- [20] Ö. Akarsu, S. Kumar, S. Sharma and L. Tedesco, Constraints on a Bianchi type I spacetime extension of the standard Λ CDM model, *Phys. Rev. D* **100**, 023532 (2019).
- [21] T. Singh, R. Chaubey, A. Singh, Bounce conditions for FRW models in modified gravity theories, *Eur. Phys. J. Plus* **130**, 31 (2015).
- [22] A. Singh, Homogeneous and anisotropic cosmologies with affine EoS: a dynamical system perspective, *Eur. Phys. J. C* **83**, 696 (2023).
- [23] V. Sahni, A. Shafieloo and A. A. Starobinsky, Two new diagnostics of dark energy, *Phys. Rev. D* **78** 103502 (2008).
- [24] S. K. Tripathy, B. Mishra, M. Khlopov and S. Ray, Cosmological models with a hybrid scale factor, *Int. J. Mod. Phys. D* **30** 2140005 (2021).
- [25] S. Mandal, A. Singh, R. Chaubey, Observational constraints and cosmological implications of NLE model with variable G , *Eur. Phys. J. Plus* **137**, 1246 (2022).
- [26] N. Myrzakulov, M. Koussour and A. Mussatayeva, Quintessence-like features in the late-time cosmological evolution of $f(Q)$ symmetric teleparallel gravity, *Chin. J. Phys.* **85**, 345–358 (2023).
- [27] M. Shahalam, S. Sami, A. Agarwal, Om diagnostic applied to scalar field models and slowing down of cosmic acceleration, *Mon. Not. R. Astron. Soc.* **448**, 2948 (2015).
- [28] B. Mishra, S.K. Tripathy and S. Ray, Cosmological models with squared trace in modified gravity, *Int. J. Mod. Phys. D* **29**, 2050100 (2020).
- [29] B. Mishra, F. MD. Esmaili, S. Ray, Cosmological models with variable anisotropic parameter in $f(R, T)$ gravity, *Ind. J. Phys.* **95**, 2245 (2021).
- [30] G. S. Sharov, S. Bhattacharya, S. Pan, R. C. Nunes and S. Chakraborty, A new interacting two-fluid model and its consequences, *Mon. Not. R. Astron. Soc.* **466**, 3497-3506 (2017).
- [31] B. Popovic, D. Brout, R. Kessler and D. Scolnic, The Pantheon+ Analysis: Forward-Modeling the Dust and Intrinsic Colour Distributions of Type Ia Supernovae, and Quantifying their Impact on Cosmological Inferences, *arXiv:2112.04456 [astro-ph.CO]*.
- [32] D. Brout *et al.*, The Pantheon+ Analysis: SuperCal-fragilistic Cross Calibration, Retrained SALT2 Light-curve Model, and Calibration Systematic Uncertainty, *Astrophys. J.* **938**, 111 (2022).
- [33] D. Scolnic *et al.*, The Pantheon+ Analysis: The Full Data Set and Light-curve Release, *Astrophys. J.* **938**, 113 (2022).